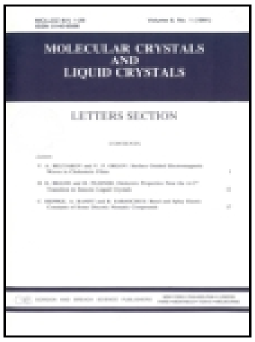

Molecular Crystals and Liquid Crystals

ISSN: 1542-1406 (Print) 1563-5287 (Online) Journal homepage: http://www.tandfonline.com/loi/gmcl20

Synthesis, characterization, and mesomorphic investigations of diester-substituted salicylaldimines and their copper (II) complexes

Sachin Kumar Singh, Madan Kumar Singh, Hemant Kumar Singh & Bachcha Singh

To cite this article: Sachin Kumar Singh, Madan Kumar Singh, Hemant Kumar Singh & Bachcha Singh (2016) Synthesis, characterization, and mesomorphic investigations of diester-substituted salicylaldimines and their copper (II) complexes, Molecular Crystals and Liquid Crystals, 624:1, 77-90, DOI: 10.1080/15421406.2015.1044196

To link to this article: http://dx.doi.org/10.1080/15421406.2015.1044196

MOL. CRYST. LIQ. CRYST.
2016, VOL. 624, NO. 1, 77–90
http://dx.doi.org/10.1080/15421406.2015.1044196

Taylor & Francis
Taylor & Francis Group

Synthesis, characterization, and mesomorphic investigations of diester-substituted salicylaldimines and their copper (II) complexes

Sachin Kumar Singh, Madan Kumar Singh, Hemant Kumar Singh, and Bachcha Singh

Department of Chemistry (Centre of Advanced Studies), Faculty of Science, Banaras Hindu University, Varanasi, India

ABSTRACT
A novel homologous series of N-[4-[4′-n-alkoxy)benzoyloxy-2-hydroxybenzylidene)-4-carbethoxy anilines, $H_{2n+1}C_nOC_6H_4C(O)OC_6H_3(OH)C(H)=NC_6H_4COOC_2H_5$ (n = 6, 8, 10, 12, 14, 16) and their copper(II) complexes have been synthesized. All these compounds have been characterized by suitable spectroscopic techniques. The mesomorphic properties of these compounds were investigated by differential scanning calorimetry (DSC) and polarizing optical microscopy (POM). The ligands exhibit wide range of enantiotropic smectic A and nematic phases as confirmed by their typical optical texture under polarizing microscope. The square planar copper(II) complexes of the ligands show only an isotropic phase at higher temperature and no mesogenic nature is observed. DFT calculations have been performed using GAUSSIAN-03 program at B3LYP level to obtain the stable electronic structure of the ligand with decyloxy chain length and its copper(II) complex.

KEYWORDS
Copper complexes; DFT study; mesophase; salicylaldimines; structure–function relationship; thermotropic liquid crystal

1. Introduction

Liquid crystals (mesogens) are fascinating functional materials and are important in the field of advanced materials such as electro-optical devices, laser addressed devices, passive block filters, and devices based on thermochromism such as fever indicators, gadgets, reflective type LCD′s, field effect transistors and sensors [1]. They are indispensable in biological systems (e.g. membranes) and are becoming part of high-tech processes [2]. The mesomorphic (liquid crystalline) behavior of an organic compound is basically dependent on its molecular architecture in which a slight change in the molecular geometry brings about considerable change in its mesomorphic properties. Detailed studies on liquid crystals have led to empirical rules which include the effect of chemical constitution in the nematogenic and smectogenic mesophases [3]. Most of these studies have been focused on Schiff bases since the discovery of 4-methoxybenzylidene-4′-butylaniline (MBBA) which exhibits a room temperature nematic phase [4]. In these organic liquid crystalline, Schiff base species whose rigid

---

CONTACT Bachcha Singh ✉ bsinghbhu@rediffmail.com, bsingh@bhu.ac.in Department of Chemistry (Centre of Advanced Studies), Faculty of Science, Banaras Hindu University, Varanasi 221005, India.
Present address for Madan Kumar Singh: Aditya Birla Science & Technology Company Ltd., MIDC Taloja, Dist. Raigad-410208, Navi Mumbai, Maharashtra, India.

Color versions of one or more of the figures in the article can be found online at www.tandfonline.com/gmcl.

core is salicylaldimines have been proved to be convenient starting materials for the preparation of metallomesogens [5]. The copper (II) complexes of salicylaldimine have been studied to establish structure–property relationship.

Ovchinnikov and coworkers [6] were the first to described the liquid crystalline properties of the complexes of the type bis [4-X-N-(4-Y-phenyl) salicylaldiminato] copper (II) with X = Y = alkoxy and studied their mesogenic properties and reported them to be smectogenic. Since then either four long alkoxy [7–10] chains or two alkoxy (= X) and two alkyl (= Y) chains 11–14] have been employed. Over the past few decades, low molar mass Schiff base esters have been investigated extensively. In these studies, the influence of a terminal alkyl chain upon the liquid crystalline properties [15,16] and the possibility of enhancing the rigidity of the Schiff base core system through metal complex formation [17,18] have been claimed as favorable pathways to improve the mesogenic properties (Fig. 1).

In order to explore further the factors which govern the thermal stability of liquid crystals with diester containing salicylaldimine core, and the relationship with its molecular structures, we carry out the investigations in a more comprehensive manner on wherein a alkoxy benzoate ester group into the aldehyde fragment of benzylideneaniline compound and ethoxybenzoate group as terminal fragment are introduced through the preparation of a homologous series of mesogenic ligands and their copper(II) complexes. The molecular structures of the title compounds were characterized by various spectroscopic techniques and their liquid crystalline behavior were investigated by differential scanning calorimetry (DSC) and polarizing optical microscopy (POM).

2. Experimental details

2.1. *Materials*

Ethyl 4-aminobenzoate, 4-hydroxybenzoic acid, 2,4-dihydroxy benzaldehyde, bromoalkanes, thionyl chloride, copper(II) acetate monohydrate purchased from Aldrich Chemicals, USA were used as received. All other solvents and reagents were purchased from Merck. The solvents were dried using standard methods [19] when required.

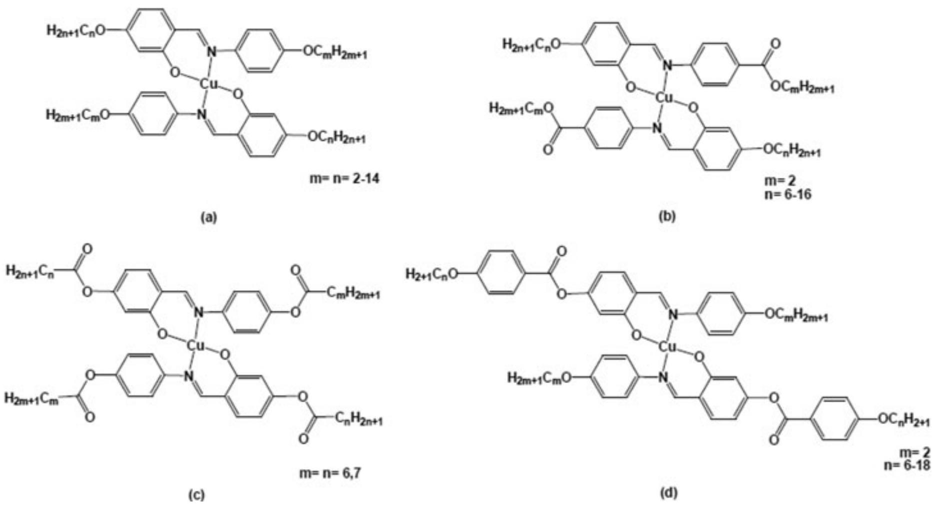

Figure 1. Mesogenic copper(II) complexes of salicylideneamine[7, 8, 11, 17].

2.2. *Techniques*

Elemental analyses were performed on a CE-440 Exeter Analytical CHN analyser. IR spectra (4000–100 cm^{-1}) were recorded on a Varian 3100 FT-IR Excalibur series spectrophotometer. ^{1}H NMR spectra were obtained on a JEOL FT-NMR AL 300 MHz spectrometer using tetramethylsilane as the internal standard. UV-visible spectra were recorded on an (UV)-1700 Pharma Spec. Shimadzu UV–visible spectrophotometer. Room temperature magnetic susceptibility measurements were performed on a Cahn Faraday balance using Co[Hg(SCN)$_4$] as standard. The magnetic susceptibility was corrected for diamagnetism using Pascal's constants. Differential scanning calorimetry thermograms were recorded with a Mettler Toledo TC 15 TA differential scanning calorimeter at the rate of 5.0 K min^{-1} under a nitrogen atmosphere using spec grade pure indium as standard by taking sample in close-lid aluminum pans. The transition temperatures from DSC thermograms have been determined with an accuracy of ±0.1 K. The mesophase type was identified by visual comparison with known phase standards using an HT 30.01 NTT 268 Lomo polarizing optical microscope fitted with a hot stage with temperature controlling accuracy of 0.1 K. Quantum chemical calculations were carried out using density functional theory (DFT) as implemented in GAUSSIAN-03 package.

2.3. *Synthesis*

The starting materials 4-alkoxybenzoic acids and 4-(4′-alkoxy)benzoyloxy-2-hydroxy benzaldehydes were prepared according to literature procedure [20].

2.3.1. *Synthesis of N-(4-(4′-n-decyloxy)benzoyloxy-2-hydroxybenzylidene)-4-carbethoxy aniline, C$_{10}$LH*

4-(4′-Decyloxy)benzoyloxy-2-hydroxybenzaldehyde (1.99 g, 5 mmol) and ethyl-4-aminobenzoate (0.97 g, 5 mmol) were mixed together in ethanol (20 mL) followed by addition of 8–10 drops of glacial acetic acid. The reaction mixture was refluxed for 4 h. The yellow precipitate that formed on cooling was filtered off, washed with cold ethanol and recrystallized from ethanol-chloroform (1/1. v/v) mixture.

All the other members of the series were prepared in a similar manner. The yield, IR, NMR, UV-Vis and elemental data for the compounds are summarized as follows.

2.3.2. *N-(4-(4′-n-hexyloxy)benzoyloxy-2-hydroxybenzylidene)-4-carbethoxyaniline, C$_6$LH*

Yield: 92%; IR (KBr, cm^{-1}): 3460(OH), 2918–2857(aliphatic C-H), 1724(ester, C(=O)OPh), 1712(ester, C(=O)OEt), 1628(–C=N), 1599, 1510(Ph), 1275, 1251(OPh); ^{1}H NMR (CDCl$_3$, TMS) δ_H (ppm): 13.53(s,1H,-OH), 8.87(s, 1H,–CH=N), 8.53–6.73(m, 11H, ArH), 4.53(q, 2H, COOC$\underline{H}_2$-), 4.20(t, 2H, -OCH$_2$), 2.20–1.20(m, 11H„-[CH$_2$]$_n$), 0.93(t, 3H, - CH$_3$).; ^{13}C NMR (75 MHz, CDCl$_3$, 25°C): δ_c 166.63, 164.14, 162.77, 152.57, 133.87, 131.01, 127.73, 120.97, 112.77, 108.01, 101.52, 77.42, 76.56, 68.32, 52.12, 31.88, 29.53, 25.96, 22.66. 14.11; UV-visible (CHCl$_3$): λ_{max} = 350, 317, 275, 259 nm; Elemental analyses: calculated for $C_{29}H_{31}NO_6$ (%), C, 71.15; H, 6.38; N, 2.92; Found, C, 71.21; H, 6.45; N, 2.80.

2.3.3. *N-(4-(4′-n-octyloxy)benzoyloxy-2-hydroxybenzylidene)-4-carbethoxyaniline, C$_8$LH*

Yield: 87%; IR (KBr, cm^{-1}): 3420(OH), 2918–2857(aliphatic C-H), 1724(ester, C(=O)OPh), 1711(ester, C(=O)OEt), 1628(–C=N), 1599–1510(Ph), 1275, 1251(OPh); ^{1}H NMR (CDCl$_3$, TMS) δ_H (ppm): 13.53(s,1H,-OH), 8.83(s, 1H,–CH=N), 8.53–6.73(m, 11H, ArH), 4.53(q, 2H, COOC$\underline{H}_2$-), 4.20(t, 2H, -OCH$_2$), 2.20–1.20(m, 15H„-[CH$_2$]$_n$), 0.93(t, 3H, - CH$_3$).; ^{13}C NMR (75 MHz, CDCl$_3$, 25°C): δ_c 166.65, 164.04, 162.79, 152.58, 133.87, 131.01, 127.73, 120.96, 112.75, 108.00, 101.51, 77.42, 76.57, 68.33, 52.12, 31.88, 29.53, 25.96, 22.66. 14.10; UV-visible (CHCl$_3$): $_{max}$ = 367, 329, 277, 270 nm; Elemental analyses: calculated for $C_{31}H_{35}NO_6$ (%), C, 71.93; H, 6.81; N, 2.70; Found, C, 71.85; H, 6.87; N, 2.74.

2.3.4. *N-(4-(4′-n-decyloxy)benzoyloxy-2-hydroxybenzylidene)-4-carbethoxyaniline, $C_{10}LH$*

Yield: 87%; IR (KBr, cm^{-1}): 3470(OH), 2906–2857(aliphatic C-H), 1724(ester, C(=O)OPh), 1711(ester, C(=O)OEt), 1628(–C=N), 1599–1510(Ph), 1275, 1253(OPh); ^{1}H NMR (CDCl$_3$, TMS) δ_H (ppm): 13.53(s,1H,-OH), 8.83(s, 1H,–CH=N), 8.53–6.73(m, 11H, ArH), 4.53(q, 2H, COOC$\underline{H}_2$-), 4.20(t, 2H, -OCH$_2$), 2.20–1.20(m, 19H„-[CH$_2$]$_n$), 0.93(t, 3H, - CH$_3$).; ^{13}C NMR (75 MHz, CDCl$_3$, 25°C): δ_c 166.64, 164.05, 162.79, 152.58, 133.88, 131.03, 127.74, 120.96, 112.74, 108.01, 101.53, 77.42, 76.57, 68.34, 52.12, 31.89, 29.53, 25.96, 22.67. 14.10; UV-visible (CHCl$_3$): λ_{max} = 357, 327, 278, 265 nm; Elemental analyses: calculated for $C_{33}H_{39}NO_6$ (%), C, 72.63; H, 7.20; N, 2.57; Found, C, 72.55; H, 7.17; N, 2.55.

2.3.5. *N-(4-(4′-n-dodecyloxy)benzoyloxy-2-hydroxybenzylidene)-4-carbethoxyaniline, $C_{12}LH$*

Yield: 87%; IR (KBr, cm^{-1}): 3472(OH), 2918–2852(aliphatic C-H), 1724(ester, C(=O)OPh), 1712(ester, C(=O)OEt), 1633(–C=N), 1602–1510(Ph), 1271, 1250(OPh); ^{1}H NMR (CDCl$_3$, TMS) δ_H (ppm): 13.53(s,1H,-OH), 8.83(s, 1H,–CH=N), 8.53–6.73(m, 11H, ArH), 4.53(q, 2H, COOC$\underline{H}_2$-), 4.20(t, 2H, -OCH$_2$), 2.20–1.20(m, 23H„-[CH$_2$]$_n$), 0.93(t, 3H, - CH$_3$).; ^{13}C NMR (75 MHz, CDCl$_3$, 25°C): δ_c 166.75, 164.14, 162.89, 152.59, 133.77, 131.08, 127.13, 120.96, 112.79, 108.00, 101.51, 77.42, 76.57, 68.33, 52.12, 31.89, 29.53, 25.97, 22.66. 14.10; UV-visible (CHCl$_3$): λ_{max} = 367, 347, 280, 263 nm; Elemental analyses: calculated for $C_{35}H_{43}NO_6$ (%), C, 73.27; H, 7.55; N, 2.49; Found, C, 73.33; H, 7.51; N, 2.53.

2.3.6. *N-(4-(4′-n-tetradecyloxy)benzoyloxy-2-hydroxybenzylidene)-4-carbethoxyaniline, $C_{14}LH$*

Yield: 87%; IR (KBr, cm^{-1}): 3474(OH), 2919–2851(aliphatic C-H), 1724(ester, C(=O)OPh), 1710(ester, C(=O)OEt), 1636(–C=N), 1602–1510(Ph), 1274, 1250(OPh); ^{1}H NMR (CDCl$_3$, TMS) δ_H (ppm): 13.53(s,1H,-OH), 8.83(s, 1H,–CH=N), 8.53–6.73(m, 11H, ArH), 4.53(q, 2H, COOC$\underline{H}_2$-), 4.20(t, 2H, -OCH$_2$), 2.20–1.20(m, 27H„-[CH$_2$]$_n$), 0.93(t, 3H, - CH$_3$).; ^{13}C NMR (75 MHz, CDCl$_3$, 25°C): δ_c 166.67, 164.24, 162.76, 152.59, 133.77, 131.09, 127.83, 120.86, 112.74, 108.01, 101.56, 77.52, 76.59, 68.36, 52.22, 31.88, 29.53, 25.96, 22.66. 14.10; UV-visible (CHCl$_3$): λ_{max} = 377, 337, 276, 260 nm; Elemental analyses: calculated for $C_{35}H_{43}NO_6$ (%), C, 73.27; H, 7.55; N, 2.49; Found, C, 73.33; H, 7.51; N, 2.53.

2.3.7. *N-(4-(4′-n-hexadecyloxy)benzoyloxy-2-hydroxybenzylidene)-4-carbethoxyaniline, $C_{16}LH$*

Yield: 87%; IR (KBr, cm^{-1}): 3474(OH), 2919–2851(aliphatic C-H), 1724(ester, C(=O)OPh), 1710(ester, C(=O)OEt), 1636(–C=N), 1602–1510(Ph), 1274, 1250(OPh); ^{1}H NMR (CDCl$_3$, TMS) δ_H (ppm): 13.53(s,1H,-OH), 8.83(s, 1H,–CH=N), 8.53–6.73(m, 11H, ArH), 4.53(q, 2H, COOC$\underline{H}_2$-), 4.20(t, 2H, -OCH$_2$), 2.20–1.20(m, 31H„-[CH$_2$]$_n$), 0.93(t, 3H, - CH$_3$).; ^{13}C NMR (75 MHz, CDCl$_3$, 25°C): δ_c 165.65, 164.07, 162.78, 152.59, 133.77, 131.11, 127.73, 120.95, 112.76, 108.01, 101.52, 77.42, 76.58, 68.32, 52.12, 31.88, 29.53, 25.97, 22.66. 14.11; UV-visible

($CHCl_3$): $\lambda_{max} = 358, 329, 276, 267$ nm; Elemental analyses: calculated for $C_{39}H_{51}NO_6$ (%), C, 74.37; H, 8.16; N, 2.22; Found, C, 74.31; H, 8.06; N, 2.28.

General procedures for preparation of copper complexes, $Cu(C_nL)_2$:

2.3.8. *Synthesis of copper(II) complex of N-(4-(4′-n-decyloxy)benzoyloxy-2-hydroxybenzy-lidene)-4-carbethoxy aniline, $Cu(C_{10}L)_2$*

To a solution (20 mL) of N-(4-(4′-n-decyloxy)benzoyloxy-2-hydroxybenzylidene)-4-carbethoxy aniline (1.14 g, 2 mmol) in hot methanol/chloroform (1/1, v/v,) stirred at room temperature was added copper acetate (0.2 g, 1 mmol) in methanol (10 mL). The mixture was stirred at room temperature for 4 h. The resulting brown solid was filtered off, washed with methanol and recrystallized from chloroform-ethanol (1/1, v/v).

All the other members of the series were prepared in a similar manner. The yield, IR, UV-Vis and elemental data for the compounds are summarized as follows.

2.3.9. *Copper(II) complex of N-(4-(4′-n-hexyloxy)benzoyloxy-2-hydroxybenzylidene)-4-carbethoxy aniline, $Cu(C_6L)_2$*

Yield: 78%; IR (KBr, cm^{-1}): 2920–2857(aliphatic C-H), 1724(ester, C(=O)OPh), 1712(ester, C(=O)OEt), 1608(−C=N), 1599–1510(Ph), 1280(OPh); UV–visible: (nujol): $\lambda_{max} = 456, 379, 280, 267, 212$; Elemental analyses: calculated for $C_{58}H_{60}N_2O_{12}Cu$ (%), C, 66.94; H, 5.81; N, 2.69; Cu, 6.10; Found, C, 66.99; H, 5.78; N, 2.73; Cu, 6.20.

2.3.10. *Copper(II) complex of N-(4-(4′-n-octyloxy)benzoyloxy-2-hydroxybenzylidene)-4-carbethoxy aniline, $Cu(C_8L)_2$*

Yield: 89%; IR (KBr, cm^{-1}): 2922–2852(aliphatic C-H), 1724(ester, C(=O)OPh), 1712(ester, C(=O)OEt), 1608(−C=N), 1599–1510(Ph), 1280(OPh); UV–visible: (nujol): $\lambda_{max} = 463, 386, 280, 222$; Elemental analyses: calculated for $C_{62}H_{68}N_2O_{12}Cu$ (%), C, 67.90; H, 6.25; N, 2.55; Cu, 5.80; Found, C, 67.88; H, 6.20; N, 2.58; Cu, 5.70.

2.3.11. *Copper (II) complex of N-(4-(4′-n-decyloxy)benzoyloxy-2-hydroxybenzylidene)-4-carbethoxy aniline, $Cu(C_{10}L)_2$*

Yield: 89%; IR (KBr, cm^{-1}): 2922–2852(aliphatic C-H), 1724(ester, C(=O)OPh), 1712(ester, C(=O)OEt), 1608(−C=N), 1599–1510(Ph), 1280(OPh);UV–visible: (nujol): $\lambda_{max} = 453, 384, 278, 212$; Elemental analyses: calculated for $C_{62}H_{68}N_2O_{12}Cu$ (%), C, 67.90; H, 6.25; N, 2.55; Cu, 5.80; Found, C, 67.88; H, 6.20; N, 2.58; Cu, 5.70

2.3.12. *Copper (II) complex of N-(4-(4′-n-dodecyloxy)benzoyloxy-2-hydroxybenzylidene)-4-carbethoxy aniline, $Cu(C_{12}L)_2$*

Yield: 89%; IR (KBr, cm^{-1}): 2922–2852(aliphatic C-H), 1724(ester, C(=O)OPh), 1712(ester, C(=O)OEt), 1608(−C=N), 1599–1510(Ph), 1280(OPh);UV–visible: (nujol): $\lambda_{max} = 454, 380, 279, 210$; Elemental analyses: calculated for $C_{70}H_{84}N_2O_{12}Cu$ (%), C, 69.54; H, 7.00; N, 2.32; Cu, 5.30; Found, C, 69.55; H, 7.06; N, 2.30; Cu, 5.20

2.3.13. *Copper (II) complex of N-(4-(4′-n-tetradecyloxy)benzoyloxy-2-hydroxybenzylide)-4-carbethoxy aniline, $Cu(C_{14}L)_2$*

Yield: 89%; IR (KBr, cm^{-1}): 2922–2852(aliphatic C-H), 1724(ester, C(=O)OPh), 1712(ester, C(=O)OEt), 1608(−C=N), 1599–1510(Ph), 1280(OPh);UV–visible: (nujol): $\lambda_{max} = 450, 387, 270, 213$; Elemental analyses: calculated for $C_{74}H_{92}N_2O_{12}Cu$ (%), C, 70.24; H, 7.33; N, 2.22; Cu, 5.03; Found, C, 70.18; H, 7.20; N, 2.18; Cu, 4.98.

2.3.14. *Copper (II) complex of N-(4-(4′-n-hexadecyloxy)benzoyloxy-2-hydroxybenzylidene)-4-carbethoxy aniline, Cu($C_{16}L)_2$*

Yield: 89%; IR (KBr, cm^{-1}): 2922–2852(aliphatic C-H), 1724(ester, C(=O)OPh), 1712(ester, C(=O)OEt), 1608(–C=N), 1599–1510(Ph), 1280(OPh);UV–visible: (nujol): $\lambda_{max} = 457$, 380, 273, 222; Elemental analyses: calculated for $C_{78}H_{100}N_2O_{12}Cu$ (%), C, 70.91; H, 7.63; N, 2.12; Cu, 4.80; Found, C, 70.95; H, 7.66; N, 2.18; Cu, 4.74.

3. Results and discussion

3.1. *Synthesis and characterization*

The synthetic route for preparation of Schiff base N-4-(4′-n-alkoxy)benzoyloxy-2-hydroxybenzylidene)4-carbethoxy anilines and their copper (II) complexes is outlined in Scheme 1.

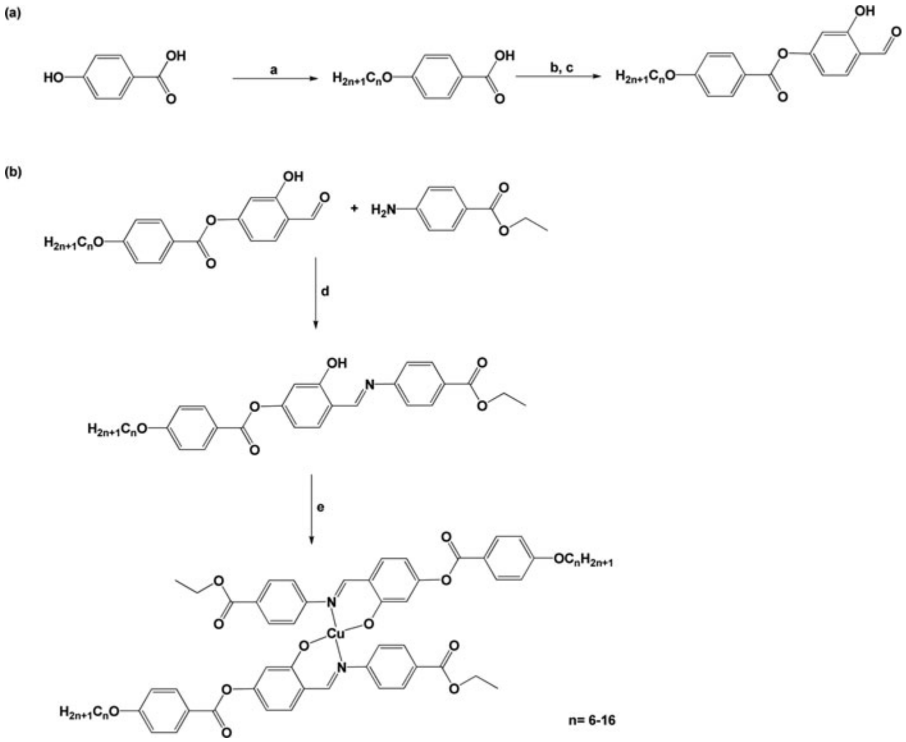

Scheme 1. *Reactions and reagents:* (a) $C_nH_{2n+1}Br$ (1.0 equiv.), KOH (3.0 equiv.), refluxing in EtOH, 7 h, (b) $SOCl_2$ (3.0 equiv.), refluxing in dry chloroform, 7 h (c) 2,4 dihydroxybenzaldehyde (1.0 equiv.), pyridine (catalyst), refluxing in dry DCM. (d) acetic acid (3 drops), refluxing in EtOH, 4 h. (e) $Cu(OAc)_2.H_2O$ (0.5 equiv.), refluxing in $EtOH/CHCl_3$ (1:1), 4 h.

Alkylation of 4-hydroxybenzoic acid with alkyl bromide in presence of strong base in ethanol allowed us to obtain a reasonable yield of 4-alkoxybenzoic acid, which on further esterification with 2, 4-dihydroxy benzaldehyde gave 4-(4′-alkoxy)benzoyloxy-2-hydroxy benzaldehyde. The Schiff base was obtained by the condensation of ethyl 4-aminobenzoate with 4-(4′-alkoxy) benzoyloxy-2-hydroxybenzaldehyde in refluxing ethanol.

The copper (II) complex was prepared by reaction of ethyl-(4-(4′-alkoxy) benzoyloxy-2-hydroxy-benzylideneamino)-benzoate with $Cu(OAc)_2.H_2O$ in stirring ethanol. The copper complex was then isolated as brown crystals by recrystallization from absolute ethanol in good yield (66–70%).

The ligands and their copper (II) complexes were characterized by elemental analyses and standard spectroscopic techniques. The IR spectrum of 4-(4′-decyloxy) benzoyloxy-2-hydroxybenzaldehyde shows absorption bands at 3408, (2925, 2853), 1714, 1678, (1605, 1512), (1304, 1255) cm^{-1} assigned to ν (OH), ν (aliphatic C-H stretch), ν (C=O phenyl ester), ν (C=O aldehyde), ν (Ph), and ν (OPh), respectively. The IR spectrum of N-[4-[4′-n-decyloxy)benzoyloxy-2-hydroxybenzylidene)-4-carbethoxy aniline shows absorption bands at 3470, (2906, 2857), 1724, 1711, 1628, (1599, 1510) and (1275, 1253) which are assigned to ν (OH), ν (aliphatic C-H), ν (C=O) of phenyl ester, ν (C=O) of ethyl ester, ν (C=N), ν (Ph) and ν (OPh) modes, respectively. The disappearance of the band at 1678 cm^{-1} due to ν (CH = O) and appearance of a new band at 1628 cm^{-1} due to ν (C=N) indicate condensation of aldehyde with amine forming Schiff base. The proton NMR of 4-(4′-decyloxy) benzoyloxy-2-hydroxybenzaldehyde exhibit peaks δ 11.23 (s), 9.88 (s), 8.12–6.87 (m), 4.06–4.02 (m), 1.84–1.26 (m), and 0.87 (t) ppm which are assigned to -OH, -CHO, ring, $-OCH_2$, $-[CH_2]_n$ and $-CH_3$ protons, respectively. The proton NMR spectrum of N-(4-(4′-n-decyloxy)benzoyloxy-2-hydroxybenzylidene)-4-carbethoxy anilines exhibits peaks at δ 13.53(s, 1 H, -OH), 8.83(s, 1H, -CH = N), 8.53–6.73(m, 11H, ring), 4.53(q, 2H, $COOCH_2$), 4.20(t, 2H, O CH_2-), 2.2–1.2(m, 19H,$-[CH_2]_n$) and 0.93 (t, 3H, - CH_3) ppm, respectively. The signals due to Schiff base formation is observed at 8.83 ppm which corresponds to *o*-hydroxy benzylidene. The signals due to three phenyl protons overlap and are observed at δ 8.53–6.63. The length of alkyl chain has no significant effect on the position of the signals due to -OH, -CH = N, ring, $-OCH_2$, $-[CH_2]_n$, and $-CH_3$ protons.

The IR spectrum of copper (II) complex $Cu(C_{10}L)_2$, shows absorption bands at (2922, 2852), 1724, 1712, 1608, (1599, 1510), and (1304, 1280) which are assigned to ν (aliphatic C-H), ν (C=O) of phenyl ester, ν (C=O) of ethyl ester, ν (C=N), ν (Ph) and ν (OPh) modes, respectively. The disappearance of the band 3470 cm^{-1} due to ν (OH) and considerable lowering in ν (C=N) indicates deprotonation of phenolic propton and coordination of ligand to copper(II) ion through the phenoxy oxygen and azomethine nitrogen.

The electronic-spectrum of the brown color copper (II) complex shows transitions at 453, 384, 278, and 212 nm. The first two bands correspond to square planar environment of the metal [21]. The remaining bands are attributed to the π- $\pi*$ and n- $\pi*$ transitions of the ligand.

3.2. DFT study

The GAUSSIAN-03 program [22] package was employed to carry out DFT [23–28] calculations at the Becke's three parameter functional and Lee, Yang and Parr correlation functional (B3LYP) level [28–30] of calculation. 6–311++G (d,p) basis set [31] was used for ground state geometry optimization and frequency calculations of the ligand ($C_{10}LH$) while for metal complex ($Cu(C_{10}L)_2$) mixed basis set [32] 6–311++G (d,p) for C, H, N atoms and LANL2DZ for copper metal is used. The internal coordinates of the system, which is used as input for GAUSSIAN-03 program was generated by the GAUSS VIEW 4.1 program [33]. The optimized structures of the ligand, $C_{10}LH$ and its copper complex, $Cu(C_{10}L)_2$ are shown in Fig. 2.

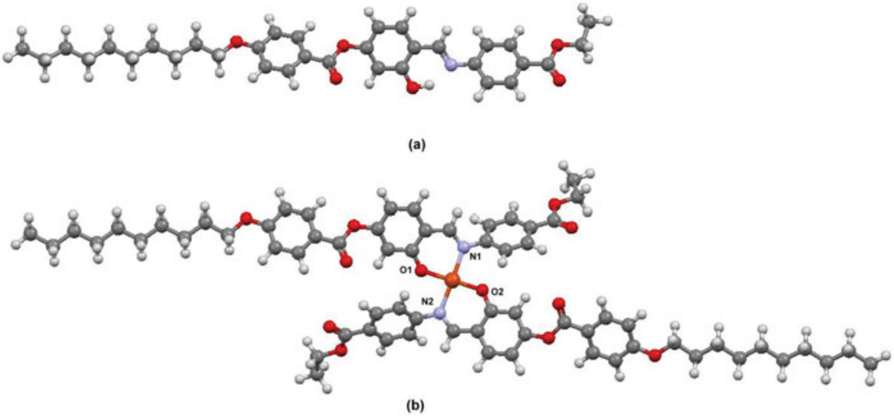

Figure 2. DFT optimized structures of (a) ligand, $C_{10}LH$ and (b) its copper(II) complex $(C_{10}L)_2Cu$.

The absence of any imaginary frequencies in the calculated vibrational frequencies ensures that the optimized geometry corresponds to a true energy minimum. The length of fully extended ligand and copper complex are found to be 33.41, 49.99 A°, respectively, from DFT calculations. All the three phenyl rings are twisted with respect to central ring in the ligand and copper complex both. For the copper complex the calculated dihedral angles between benzene rings are as follow: C(131)-C(127)-C(137)-C(130), 132.69°; C(131)-C(27)-C(118)-C(116), 148.42; C(21)-C(17)-C(30)-C(32), 125.88; C(21)-C(17)-C(3)-C(4), 146.77°. The above calculations implying twist of two outer most phenyl rings with respect to central ring.

Some of the selective geometric parameters of the optimized $Cu(C_{10}L)_2$ complex, evaluated by DFT calculation at B3LYP/6–311++G (d,p) + LANL2DZ level are shown in Table 1.

From DFT study, it has been found that the complex has average Cu–O1, Cu–N1, Cu–O2, Cu–N2 bond lengths of 1.86, 2.08, 2.00 and 2.10 Å respectively, and bond angles 92.350° and 87.670° for O(1)– Cu –N(1) and N(2)– Cu –O(2), respectively, which matched well with the other related copper salicylaldimine complex [11b].

In general, the molecular shape of 4-(benzoyloxy)salicylaldimine complexes derived from 2,4-dihydroxybenzaldehyde, can be envisaged as two rod-like structures joined by a central group and smectic C and nematic phases were identified for the copper(II) complexes of such type [2a].

Table 1. Selected bond length and bond angles[a] of $Cu(C_{10}L)_2$, from DFT study.

Structure parameter	Distance/angles
Cu–O(1)	1.859
Cu –O(2)	2.002
Cu –N(1)	2.087
Cu –N(2)	2.101
O(1)– Cu –O(2)	162.500
N(1)– Cu –N(2)	162.304
N(1)– Cu –O(2)	85.275
O(1)– Cu –N(1)	92.350
O(1)– Cu –N(2)	89.514
N(2)– Cu –O(2)	87.670

[a] Bond lengths are reported in Å and bond angles in degrees.

Table 2. Thermal Transitions and Corresponding Thermodynamic Parameters of C_6LH- C_{16}LH.

		T, °C [ΔH, kJ/mol; ΔS, J/(mol K)]	
no.	Compounds	Heating	Cooling
1	C_6LH	k 103.4 (32.8; 87.1) SmA 139.7 (3.4; 8.2) i	i 116.4 (−3.1; −7.9) SmA 61.9 (−19.9; −59.5) k
2	C_8LH	k 100.9 (40.3; 107.7) SmA 162.2 (4.4; 10.1) i	i 156.0 (−4.2; −9.8) SmA 66.9 (−31.2; −91.8) k
3	C_{10}LH	k 98.4 (50.8; 136.7) SmA 180.4 (2.3; 5.1) i	i 171.6 (−2.1; −4.7) SmA 61.9 (−35.5; −106.0) k
4	C_{12}LH	k^1 61.4 (5.1; 15.1) k^2 100.5 (40.8; 109.2) SmA 157.5 (3.2; 7.4) N 187.0 (7.7; 16.7) i	i 185.7 (6.4; 13.9) N 150.3 (2.1; 4.8) SmA 60.1 (6.7; 20.1) k
5	C_{14}LH	k^1 64.3 (5.3; 15.7) k^2 103.6 (38.7; 102.7) SmA 183.6 (3.3; 7.2) N 195.2 (6.7; 14.3) i	i 184.3 (6.3; 13.7) N 178.6 (3.1; 6.8) SmA 60.2 (30.7; 92.1) k
6	C_{16}LH	k^1 76.2 (1.5; 4.3) k^2 105.4 (70.3; 185.7) SmA 191.2 (3.4; 7.3) N 200.3 (7.1; 15.0) i	i 194.5 (6.3; 13.5) N 184.9 (2.3; 5.0) SmA 71.7 (44.6; 129.3) k

k = crystal; SmA = smectic A; N = nematic; i = isotropic liquid phases. The transition temperatures (°C), enthalpies, and entropies are determined by DSC at the scan rate of 5°C/min.

3.3. *Mesomorphic behavior*

The liquid crystalline properties of N-(4-(4′-n-alkoxy)benzoyloxy-2-hydroxybenzylidene)-4-carbethoxy anilines (C_6LH→ C_{16}LH) and their copper (II) complexes were investigated by polarizing optical microscope (POM) using a heating and cooling stage. The phase transition temperatures and enthalpies were measured by carrying out DSC thermal analysis. The phase transition temperatures, enthalpy and entropy values for the azines are summarized in Table 2. The symbols k, SmA, N and i denote crystalline, smectic A, nematic and isotropic phase, respectively.

The DSC thermograms of the hexyloxy derivatives of the series, N-(4-(4′-n-hexyloxy)benzoyloxy-2-hydroxybenzylidene)-4-carbethoxy anilines (C_6LH) shown in Figure 3 show two endothermic peaks at 103.4 ($\Delta H = 32.8$ kJmol^{-1}) and 139.7°C ($\Delta H =$ 0.4 kJmol^{-1}) in heating cycle and two exothermic peaks at 116.4 ($\Delta H = 0.1$ kJmol^{-1}) and

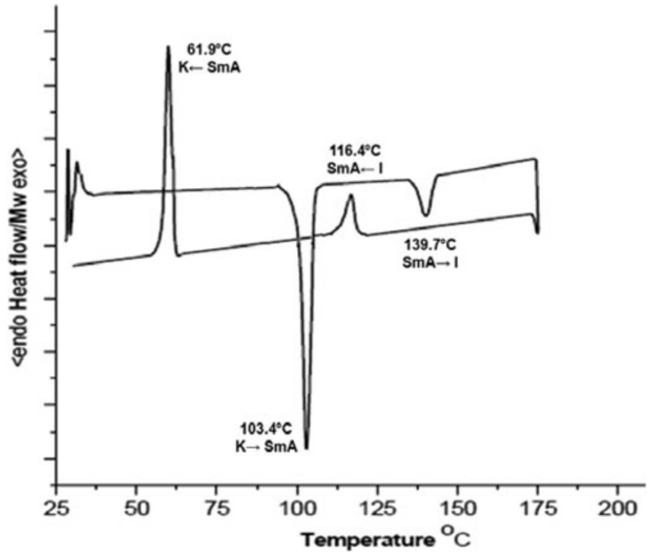

Figure 3. DSC thermogram of C_6LH.

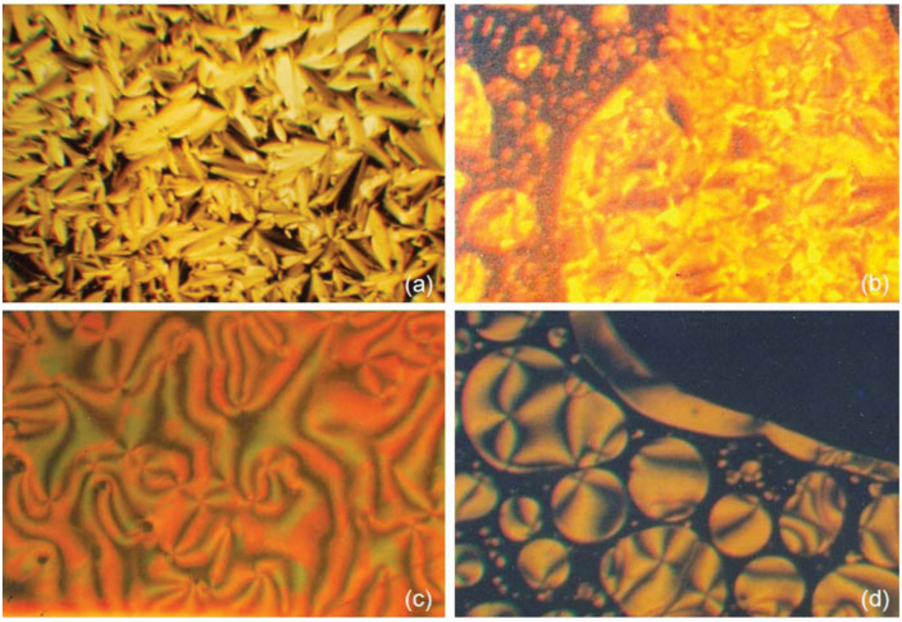

Figure 4. Microphotographs of the compounds C_nLH in heating cycle (a) broken fan texture of SmA mesophase of C_6LH at 130.1°C (b) SmA to nematic phase transition of $C_{12}LH$ at 157.5°C (c) schlieren texture of nematic mesophase of $C_{12}LH$ at 178.3°C (d) nematic to isotropic phase transition of $C_{12}LH$ at 182.1°C.

61.9°C ($\Delta H = 19.9$ kJmol^{-1}) in cooling cycle. The two endothermic peaks observed for this compound define crystal → mesophase and mesophase → isotropic (I) phase transitions respectively.

The exothermic peaks reveal an isotropic → mesophase transition and mesophase → crystal phase transition, respectively. The texture of the mesophase seen through polarizing microscope is signature of SmA mesophase, which has fluid property with higher viscosity and stratified structures with well-defined interlayer spacing. The interlayer attractions are weak and the layers are able to slide over one another relatively easily. The flexibility of the layers leads to distortions, which give rise to beautiful optical patterns known as the focal-conic texture. The molecules are aligned parallel to the layer normal, maintaining long-range orientational order and short-range positional order, which lead to the SmA mesophase. The molecular packings are found to be random for this SmA phase. A focal-conic texture is seen for this compound through optical microscopy (Fig. 4a). The appearance of smectic A phase may be arising due to the additional intramolecular forces between the phenolic OH group and nitrogen atom in the azines. Thus focal –conic texture is seen for this compound under optical microscopy, which confirms the smectic A mesophase. The similar phase transitions with similar textural pattern are shown by the next two higher members of the series with octyloxy and decyloxy chain length (C_8LH and $C_{10}LH$).

In the first heating scan of $C_{12}LH$, four sharp peaks appear at 61.4, 100.5, 157.5, and 187.0°C. The DSC thermogram recorded in the cooling scan exhibits three separate peaks at 185.7, 150.3 and 60.1°C (Fig. 5). POM observations reveal that upon heating from crystal state to 100.5°C, focal conic textures corresponding to SmA mesophase emerges. Further heating of the compound at 157.5°C leads to formation of nematic phase (Fig. 4b). The texture for compound $C_{12}LH$ between crossed polarizer resulting from surface orientation of

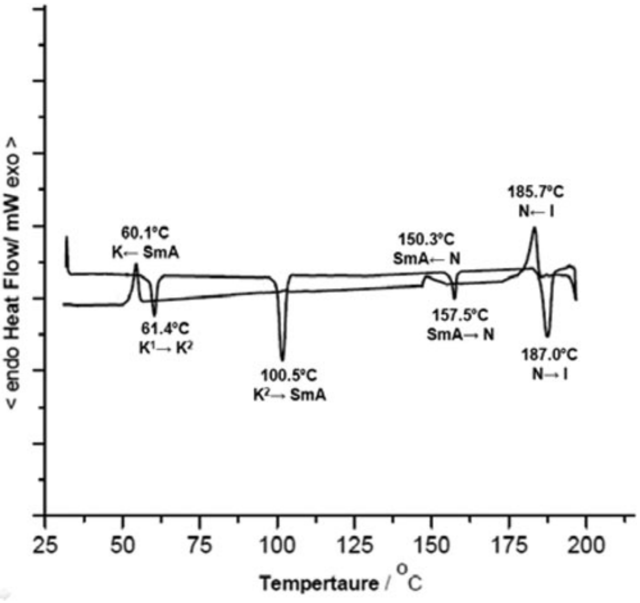

Figure 5. DSC thermogram of $C_{12}LH$.

the director of the boundaries of the sample and by defects formed in the sample shows a network of black brushes connecting center of points and line defects giving rise to disclination lines which are defect in molecular orientational order. These disclination lines are producing schlieren optical texture in nearly vertical orientation whose projection are seen as dark points with 2–4 emerging dark stripes or brushes (Fig. 4c). These black brushes are located in region where the director lies in the plane of polarization of the polarizer or analyzer. Further, heating of the compound at 187°C leads to clearing (isotropization) of the compound (Fig. 4d). It thus becomes clear that the peak at 61.4°C observed in DSC heating scan is due to crystal transformation from one state to another (k–k transition); such polymorphism has often been observed in Schiff's base containing compounds [34]. In cooling cycle, the isotropic phase changes to nematic phase at 185.7°C, which further transits to a stratified structure with well defined inter layer spacing SmA mesophase with ordered hexagonal structure at 150.3°C and finally transits to solid crystalline phase at 60.1°C. Thus, this compound exhibits enantiotropic smectic A to nematic mesophase transition. Similar phase transitions and smectic A to nematic mesophase transitions in both heating and cooling cycle showing similar textural patterns are observed for the compounds $C_{14}LH$ and $C_{16}LH$ also.

The isotropization temperature (T_i) of these ester series of compounds is found to be continuously increasing with increase in alkoxy chain length ($C_6LH \rightarrow C_{16}LH$) but melting temperature (T_m) is found to be almost constant, resulting a continuous increase in mesophase thermal stability along with higher members of the series. (Fig. 6)

The thermotropic smectic and nematic mesophase pattern based on the structural correlation of these compounds reveals a calamitic (rod like) shape for all the homologues of the series. The presence of ester linker moiety between the two phenyl groups plays a major role for the emergence of nematic mesophase in these series of compounds. It is known that the presence of ester bridging group increases flexibility and mobility of particular parts of liquid crystal molecule and hence affects the type of mesophase and its temperature range [2]. The study based on N-salicylidene with ether bridging moiety has revealed to the emergence of nematic and smectic A mesophases [7–14]. The substitution of ether linkage with the ester

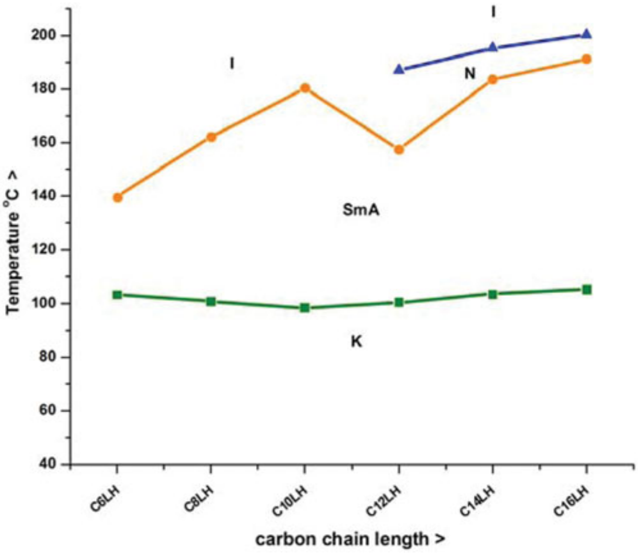

Figure 6. Phase diagram of the mesogenic ligands, C_nLH.

moiety along with the incorporation of aromatic ring with long alkoxy chain results in suppression of smectic A mesophase and leads to the occurrence of nematic phase in higher homologs of the series. Thus, it may be concluded that by the replacement of –OR with –OOC–C_6H_4–OR, the mesophase thermal stability of the system increases but order of the system decreases.

The copper(II) complexes of N-(4-(4′-n-alkoxy)benzoyloxy-2-hydroxybenzylidene)-4-carbethoxy anilines were found to be non-mesogenic with almost same clearing temperature independent of the carbon chain length. Thus in the metal complexes, chain length plays no role on isotropic temperature and polymorphism. This is probably due to fact that presence of tilted ethoxy-benzoate group in imine moiety considerably broadens the molecular width (Fig. 3). Moreover, the ester containing benzylidene ring is not coplanar with the central ring containing metal ion as depicted by DFT studies. This broadening of molecular width and the non coplanarity of the imine ring is less favorable for exhibiting liquid crystal properties of copper(II) complexes. Therefore terminal alkoxy ester bond adversely affects the mesophase formation in such ester substituted salicyldimine metal complexes. The copper complexes of substituted imine derivatives without alkoxy ester end group of the same core (salicyldimine) and same alkoxy chain length ($n = 2$) are showing SmA mesophase with high thermal stability [11b].

4. Conclusions

A new series of ester containing Schiff base derivatives having terminal alkoxy chains ($n = 6–16$) and their copper (II) complexes has been synthesized. The lower member of the series ($n = 6–10$) shows enatiotropic SmA mesophase while higher members enatiotropic SmA to nematic mesophase transition with good thermal stabilities. The copper(II) complexes are nonmesogenic in nature. Thus, addition of diester bond at salicyldeneaniline ring helps in inducing mesogenic property in the ligands and also their thermal stability but it is unfavorable for mesomorphic properties of the metal complexes due to non-coplanarity of the ester benzoate ring and also ethoxy ester end group which broadens the molecular width leading to transition of the molecule in higher order state i.e. solid state.

Acknowledgments

HKS is grateful to Council of Scientific and Industrial Research (CSIR), New Delhi, India, for providing research fellowship. Financial assistance provided by DRDO, India (Project No. ERIP/ER/1203053/M/01/1542) is gratefully acknowledged.

References

[1] (a) Venkatesan, K., & Muller, P. (2008). *J. Mat. Chem.*, *18*, 400. (b) Seredyuk, M., Gasper, A. B., & Reiman, S. (2006). *Chem. Mater.*, *18*, 2513. (c) Liao, C. T., & Wang, Y. J. (2007). *Tetrahedron*, *63*, 12437. (d) Sago, K. K., & Fujita, A. (2007). *Mol. Cryst. Liq. Cryst.*, *479*, 151. (e) Chulson, K., Park, D. J., & Kim, Y. B. (2007). *Mol. Cryst. Liq. Cryst.*, *479*, 81. (f) Bhattacharya, S. S., Rahman, M., & Mukherjee, A. (2008). *Appl. Phys. Lett.*, *92*, 122909. (g) Vasconcelos, U. B., & Schrader, A. (2008). *Tetrahedron*, *64*, 4619. (h) Lee, J. H., Mehoic, S., & Pate, B. D. (2006). *J. Mater. Chem.*, *16*, 2785.

[2] (a) Serrano, J. L. (1996). *Metallomesogens; Synthesis, Properties, and Applications*, VCH: New York. (b) Kumar, S. (2010). *Chemistry of Discotic Liquid Crystals: From Monomers to Polymers*, CRC Press: New York. (c) Stewart, G. T. (2003). *Liq. Cryst.*, *30*, 541. (d) Stewart, G. T. (2004). *Liquid Cryst.*, *31*, 443.

[3] (a) Gray, G. W. (1962). *Molecular Structure and the Properties of Liquid Crystals*, Academic Press: London. (b) Singh, S. K., Vikram, K., & Singh, B. (2011). *Liq Cryst.*, *38* (9), 1117.

[4] Kelker, H., & Scheurle, B. (1969). *Angew. Chem. Int. Edn.*, *81*, 903.

[5] Hoshino, N. (1998). *Coord. Chem. Rev.*, *174*, 77.

[6] Ovchinnikov, I. V., Galyametdinov, Y. G., Ivanova, G. I., & Yagfarova, L. M. (1984). *Dokl. Akad. Nauk SSR*, *276*, 126.

[7] (a) Ovchinnikov, I. V., Galyametdinov, Yu. G., & Bikchantaev, I. O. (1989). *Izv. Akad. Nuuk SSSR Ser. Fiz.*, *53*, 1870. (b) Bikchantaev, I. G., Galyametdinov, Yu. G., & Ovchinnikov, I. V. (1987). *Zh. Strukt. Khim.*, *28*, 61. (c) Ovchinnikov, I. V., Bikchantaev, I. G., Galyametdinov, Yu. G., & Galimov, R. M. (1988). 24th Ampere congress, Poznan.

[8] Caruso, U., Roviello, A., & Sirigu, A. (1988). *Liq. Cryst.*, *3*, 1515.

[9] Carfagna, C., Caruso, U., Roviello, A., & Sirigu, A. (1987). *Macromol. Chem. Rapid Commun.*, *8*, 345.

[10] Alonso, P. J. *et al.* (1993). *Liq. Cryst.*, *13*, 585.

[11] (a) Ghedini, M., Morrone, S., Gatteschi, D., & Zanchini, C.*Chem. Mater.*, *3*, 752. (b) Hoshino, N., Murakami, H., Matsumaza, Y., Inabe, T. I., & Maruyama, Y. (1990). *Inorg. Chem.*, *29*, 1177.

[12] Ghedini, M. *et al.* (1988). *J. Mol. Liq.*, *38*, 207.

[13] Ghedini, M. *et al.* (1987). *Mol. Cryst. Liq. Cryst.*, *151*, 75.

[14] Torquati, G. *et al.* (1990). *II Nuovo Cimento*, *12D*, 1363.

[15] Dave, J. S., & Kurian, G. (1977). *Mol. Cryst. liq. Cryst.*, *42*, 175.

[16] Matsunaga, Y., & Miyajima, N. (1990). *Mol. Cryst. Liq. Cryst.*, *178*, 157.

[17] (a) Singh, B., Singh, M. K., Dhar, R., & Srivastava, A. K. (2004). *Mol. Cryst. Liq. Cryst.*, *411*, 29. (b) Caruso, U., Roviello, A., & Sirigu, A. (1988). *Liq. Cryst.*, *3*, 1515.

[18] (a) Hoshino, N., Takashi, K., Sekiuchi, T., Tanaka, H., & Matsunaga, Y. (1998). *Inorg. Chem.*, *37*, 882. (b) Tian, Y. *et al.* (1996). *Liq. Cryst.*, *20*, 139.

[19] Riddick, J. A., Bunger, N. B., & Sanako, T. K., (1986). *Organic Solvents, Physical Properties and Methods of Purification (Techniques of Chemistry)*, 4th ed. Wiley–Interscience: New York.

[20] Singh, M. K., Singh, B., Dhar, R., & Agrawal, V. K. (2005). *Phase Transitions*, *78*(6), 495.

[21] Nicholls, D. (1973). In: *Comprehensive Inorganic Chemistry*, Chapter 42, Pergamon Press: Oxford, 31983, 1109.

[22] Frisch, M. J., *et al.* (2003). *Gaussian 03, Revision A.1*, Gaussian, Inc.: Pittsburgh.

[23] Hohenberg, P., & Kohn, W. (1964). *Phys. Rev. B.*, *136*, 864.

[24] Kohn, W., & Sham, L. J. (1965). *Phys. Rev. A.*, *140*, 1133.

[25] Becke, A. D. (1988). *Phys. Rev. A.*, *38*, 3098.
[26] Becke, A. D. (1992). *J. Chem. Phys.*, *96*, 2155.
[27] Becke, A. D. (1992). *J. Chem. Phys.*, *97*, 9173.
[28] Becke, A. D. (1993). *J. Chem. Phys.*, *98*, 5648.
[29] Lee, C., Yang, W., & Parr, R. G. (1988). *Phys. Rev. B.*, *37*, 785.
[30] Ditchfield, R., Hehre, W. J., & Pople, J. A. (1971). *J. Chem. Phys.*, *54*, 724.
[31] Hehre, W. J., Ditchfield, R., & Pople, J. A. (1972). *J. Chem. Phys.*, *56*, 2257.
[32] Dziembowska, T. *et al.* (2003). *J. Spectrochim. Acta Part A, 59*, 2175.
[33] Dennington II, R. *et al.* (2003). *Gauss View 03*, Semichem, Inc.: Shawnee Mission, KS.
[34] (a) Collings, P. J., & Hird, M. (1998). *Introduction to Liquid Crystals Chemistry and Physics*, Taylor and Francis: London. (b) Galewaki, Z. (1994). *Mol. Cryst. Liq. Cryst.*, *249*, 43.